Electronic Supplementary Material (ESI) for Inorganic Chemistry Frontiers.

Supporting Information

Centrosymmetric $Rb[Te_2O_4(OH)_5]$ and noncentrosymmetric $K_2[Te_3O_8(OH)_4]$: metal tellurates with corner and edge-sharing $(Te_4O_{18})^{12-}$ anion group

Dandan Wang,[a] Pifu Gong,[b] Xinyuan Zhang,*[a] Zheshuai Lin,[b] Zhanggui Hu *[a] and Yicheng Wu [a]

[a] Tianjin Key Laboratory of Functional Crystal Materials, Institute of Functional Crystals, Tianjin University of Technology, Tianjin 300384, China.

[b] Key Laboratory of Functional Crystals and Laser Technology, Beijing Center for Crystal Research and Development, Technical Institute of Physics and Chemistry, Chinese Academy of Sciences, Beijing 100190, China.

Contents.

Supplementary Tables.

Table S1. Fractional atomic coordinates ($\times 10^4$) and equivalent isotropic displacement parameters ($Å^2 \times 10^3$) of $Rb[Te_2O_4(OH)_5]$ (**RTOH**).

Atom	x	y	z	$U_{(eq)}{}^a$
Te1	4694.2(12)	1865.2(7)	6107.1(4)	9.63(19)
Te2	3669.0(12)	4130.2(7)	4263.0(4)	8.26(18)
Rb1	-111(2)	3997.2(11)	7844.6(6)	19.1(3)
O1	1814(13)	2456(7)	6512(4)	14.9(16)
O2	6172(14)	1204(8)	7165(4)	14.3(17)
O3	3251(12)	2370(7)	5000(4)	9.6(15)
O4	3280(13)	-215(7)	5858(4)	13.2(17)
O5	7640(14)	1199(8)	5760(4)	13.6(17)
O6	5989(12)	3966(7)	6390(4)	12.0(16)
O7	369(13)	4040(8)	3823(4)	13.5(16)
O8	4501(12)	2795(7)	3483(4)	11.3(16)
O9	3028(13)	5543(7)	5166(4)	9.7(15)

$^a U_{(eq)}$ is defined as one-third of the trace of the orthogonalized U_{ij} tensor.

Table S2. Anisotropic displacement parameters ($Å^2 \times 10^3$) for **RTOH**.

Atom	U_{11}	U_{22}	U_{33}	U_{23}	U_{13}	U_{12}
Te1	10.7(4)	9.4(3)	8.9(3)	0.6(3)	1.7(3)	-0.3(3)
Te2	9.7(4)	8.4(3)	6.4(3)	-0.3(3)	0.5(3)	-0.2(3)
Rb1	20.7(7)	18.2(6)	18.0(5)	-1.5(4)	1.3(5)	1.4(5)
O1	14(2)	17(2)	14(2)	-0.7(17)	4.8(18)	0.7(17)
O2	15(2)	15(2)	12(2)	2.4(18)	2.2(18)	2.5(18)
O3	11(2)	11(2)	7(2)	2.8(17)	2.0(17)	-1.9(17)
O4	20(5)	3(3)	17(4)	2(3)	4(3)	0(3)
O5	12(2)	15(2)	13(2)	-0.7(17)	-0.1(18)	3.4(17)
O6	16(4)	7(3)	12(3)	3(3)	-1(3)	-1(3)
O7	4(4)	22(4)	14(4)	-4(3)	-2(3)	0(3)
O8	13(4)	11(3)	11(3)	-3(3)	3(3)	-1(3)
O9	9(2)	11(2)	10(2)	-1.4(17)	3.5(17)	0.4(17)

Table S3. Selected bond lengths (Å) of **RTOH**.

Bond	Length/Å
Te1-O1	1.917(7)
Te1-O2	1.895(7)
Te1-O3	1.924(6)
Te1-O4	1.933(6)
Te1-O5	1.926(8)
Te1-O6	1.934(6)
Te2-O3	1.943(6)
Te2-O6[4]	1.945(6)
Te2-O7	1.903(7)
Te2-O8	1.814(6)
Te2-O9	1.971(6)
Te2-O9[4]	1.984(7)
Rb1-O1	2.890(7)
Rb1-O1[9]	3.274(6)
Rb1-O2[8]	3.230(7)
Rb1-O2[10]	2.899(8)
Rb1-O4[9]	3.057(7)
Rb1-O5[10]	3.105(7)
Rb1- O6[8]	3.001(7)
Rb1-O7[6]	3.176(7)
Rb1-O7[7]	2.996(6)
Rb1-O8[7]	3.059(7)

[1]1-X,-1/2+Y,3/2-Z; [2]1+X,+Y,+Z; [3]-X,-1/2+Y,3/2-Z; [4]1-X,1-Y,1-Z; [5]+X,1/2-Y,-1/2+Z; [6]-X,1-Y,1-Z; [7]+X,1/2-Y,1/2+Z;[8]-1+X,+Y,+Z; [9]-X,1/2+Y,3/2-Z; [10]1-X,1/2+Y,3/2-Z

Table S4. Selected bond angles (°) of **RTOH**.

Angle	(°)	Angle	(°)
O1-Te1-O3	90.4(3)	O3-Te2-O9[4]	90.2(3)
O1-Te1-O6	89.7(3)	O3-Te2-O9	86.1(3)
O1-Te1-O4	87.6(3)	O3-Te2-O6[4]	174.3(3)
O1-Te1-O5	176.6(3)	O6[4]-Te2-O9	88.2(3)
O2-Te1-O3	175.4(3)	O6[4]-Te2-O9[4]	89.0(3)
O2-Te1-O6	86.8(3)	O7-Te2-O9[4]	171.7(3)
O2-Te1-O4	92.5(3)	O7-Te2-O9	91.6(3)
O2-Te1-O1	92.3(3)	O7-Te2-O6[4]	89.8(3)
O2-Te1-O5	84.4(3)	O7-Te2-O3	90.1(3)
O3-Te1-O6	96.9(3)	O8-Te2-O9[4]	95.3(3)
O3-Te1-O4	83.9(3)	O8-Te2-O9	175.2(3)
O3-Te1-O5	92.8(3)	O8-Te2-O3	92.4(3)
O4-Te1-O6	177.2(3)	O8-Te2-O6[4]	93.2(3)
O5-Te1-O6	91.1(3)	O8-Te2-O7	93.0(3)
O5-Te1-O4	91.6(3)	O9-Te2-O9[4]	80.2(3)

[1]1-X, -1/2+Y, 3/2-Z; [2]1+X, +Y, +Z; [3]-X, -1/2+Y, 3/2-Z; [4]1-X, 1-Y, 1-Z; [5]+X, 1/2-Y, -1/2+Z; [6]-X, 1-Y, 1-Z; [7]+X, 1/2-Y, 1/2+Z; [8]-1+X, +Y, +Z; [9]-X, 1/2+Y, 3/2-Z; [10]1-X, 1/2+Y, 3/2-Z

Table S5. The measured SHG responses of tellurates (VI) containing alkali/alkaline earth metal or hydroxy.

Compounds	Space group	SHG effect	Band gap	PM/NPM[a]	Ref
Li_2ZrTeO_6	*R*3	2.5 × KDP	4.08 eV	PM	1
Li_2HfTeO_6	*R*3	2.2 × KDP	3.98 eV	PM	2
Li_2TiTeO_6	*P*nn2	26 × KDP	3.67 eV	PM	3
Li_2SnTeO_6	*P*nn2	2.5 × KDP	4.0 eV	PM	3
$Sr_3Zn_3TeP_2O_{14}$	*P*321	2.8 × KDP	5.58 eV	PM	4
$Ba_3Zn_3TeP_2O_{14}$	*P*321	3 × KDP	5.69 eV	PM	4
$Pb_3Mg_3TeP_2O_{14}$	*P*321	13.5 × KDP	4.96 eV	PM	5
$Bi_3TeO_6OH(NO_3)_2$	$P2_1$	3 × KDP	3.59 eV	PM	6
$Pb_9Te_2O_{13}(OH)(NO_3)_3$	$P4_32_12$	1.2 × KDP	3.62 eV	NPM	7
KTOH	*F*dd2	0.6 × KDP	4.05 eV	PM	This work

a: PM: Phase-Matching, NPM: No Phase-Matching.

Supplementary Figures.

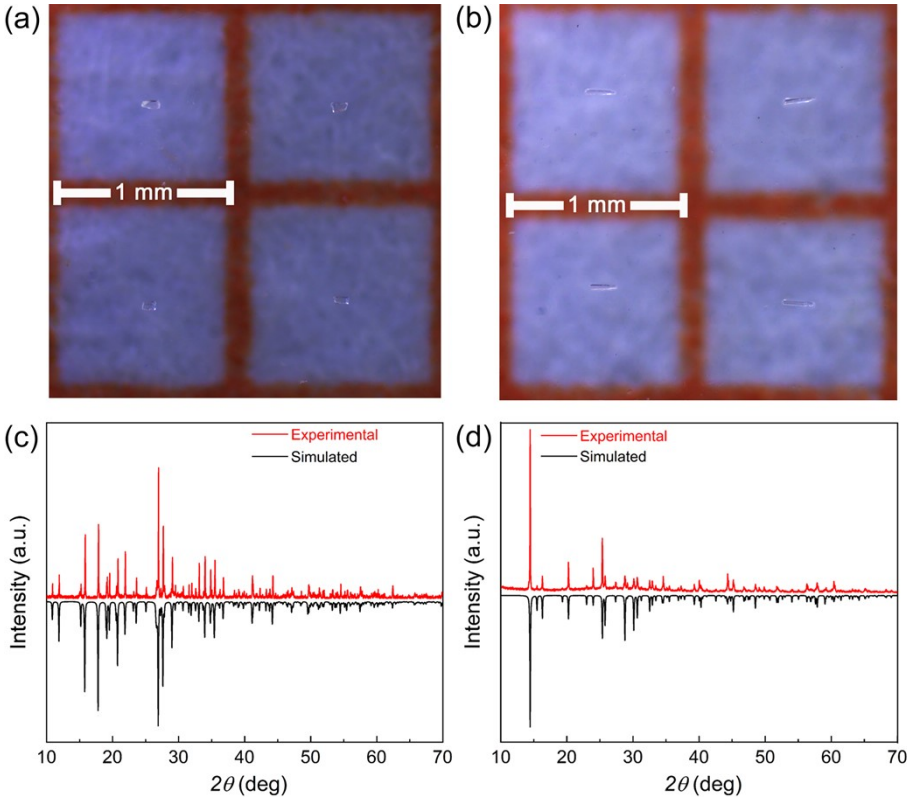

Figure S1. Crystal imagines and X-ray powder diffraction pattern of **RTOH** (a, c) and **KTOH** (b, d).

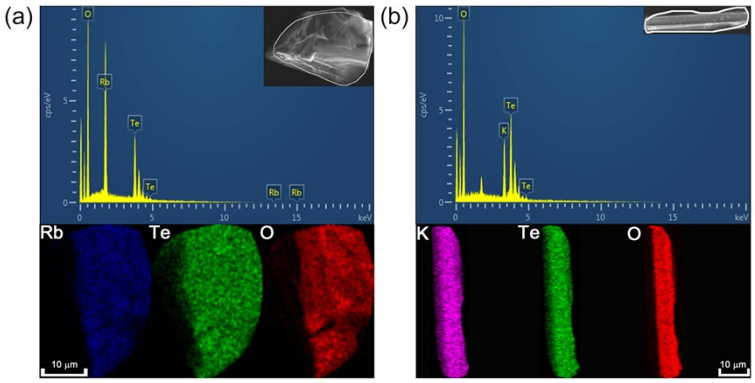

Figure S2. The EDS spectra of **RTOH** (a) and **KTOH** (b).

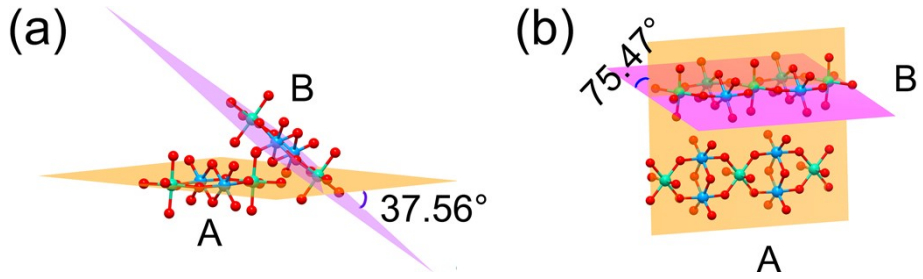

Figure S3. The dihedral angle of two $(Te_4O_{18})^{12-}$ cluster group in **RTOH** (a) and $_\infty(Te_3O_{12})^{6-}$ anionic group in **KTOH** (b).

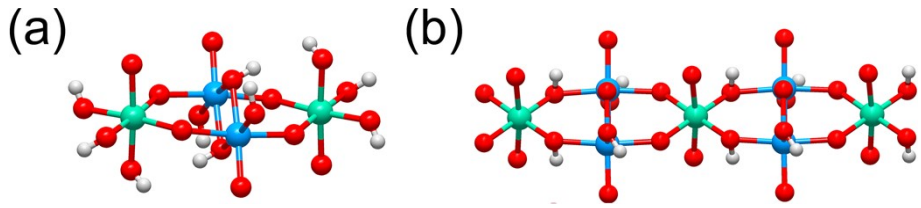

Figure S4. The $(Te_4O_{18}H_{10})^{2-}$ anionic group of **RTOH** (a) and $_\infty(Te_3O_{12}H_4)^{2-}$ anion group of **KTOH** (b).

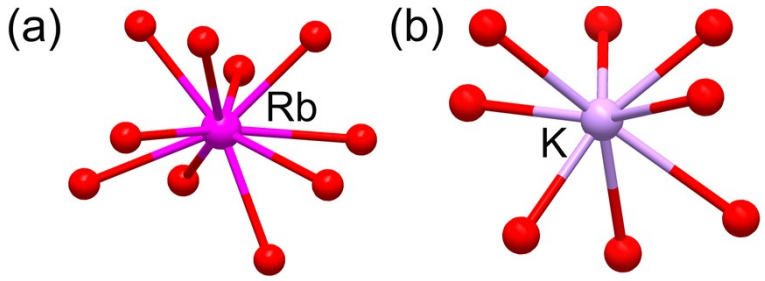

Figure S5. The coordination environment of Rb atom in **RTOH** (a) and K atom in **KTOH** (b).

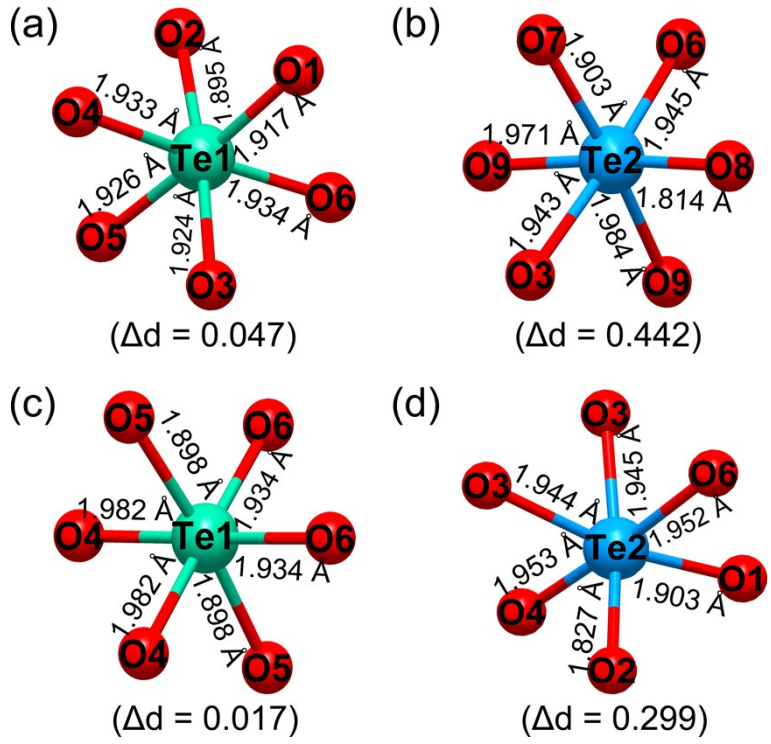

Figure S6. The bond lengths of TeO_6^{6-} polyhedra for **RTOH** (a, b) and **KTOH** (c, d).

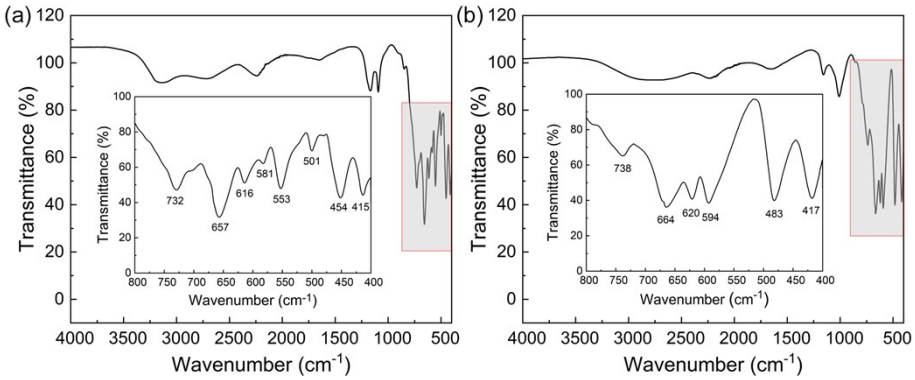

Figure S7. The IR spectra of **RTOH** (a) and **KTOH** (b).

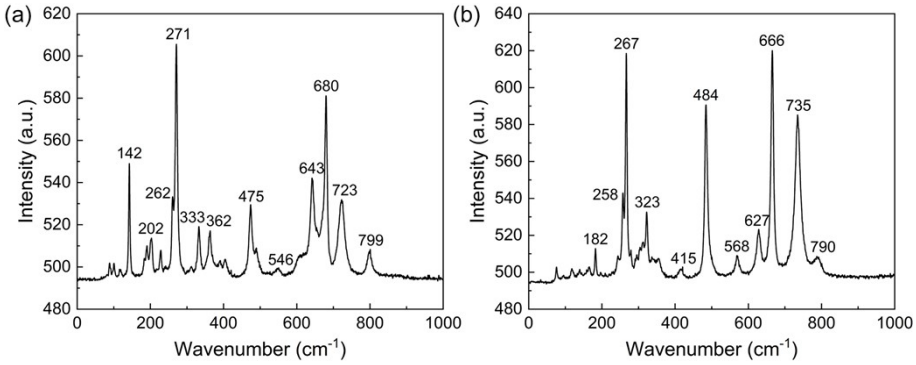

Figure S8. The Raman spectra of **RTOH** (a) and **KTOH** (b).

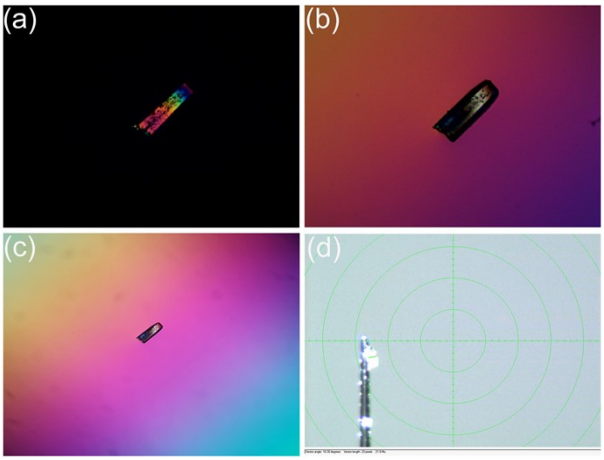

Figure S9. Birefringence measurement of **RTOH**; (a) the original crystal; (b) the crystal in the extinction state; (c) the crystal interference color observed under the microscope and (d) the photographs of crystal thickness.

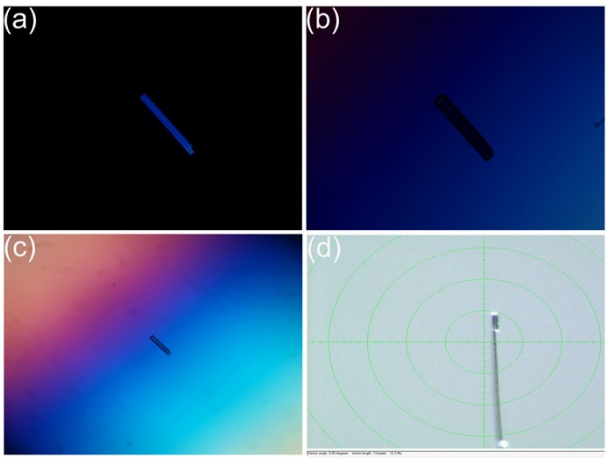

Figure S10. Birefringence measurement of **KTOH**; (a) the original crystal; (b) the crystal in the extinction state; (c) the crystal interference color observed under the microscope and (d) the photographs of crystal thickness.

References

1. W. Q. Lu, Z. L. Gao, X. T. Liu, X. X. Tian, Q. Wu, C. G. Li, Y. X. Sun, Y. Liu and X. T. Tao, Rational Design of a $LiNbO_3$-like Nonlinear Optical Crystal, Li_2ZrTeO_6, with High Laser-Damage Threshold and Wide Mid-IR Transparency Window, *J. Am. Chem. Soc.*, 2018, **140**, 13089-13096.
2. D. Wang, Y. X. Zhang, Q. Shi, Q. Liu, D. Q. Yang, B. B. Zhang and Y. Wang, Tellurate polymorphs with high-performance nonlinear optical switch property and wide mid-IR transparency, *Inorg. Chem. Front.*, 2022, DOI: 10.1039/d2qi00200k.
3. X. L. Du, X. J. Guo, Z. L. Gao, F. A. Liu, F. F. Guo, S. Y. Wang, H. Y. Wang, Y. X. Sun and X. T. Tao, Li_2MTeO_6 (M=Ti, Sn): Mid-Infrared Nonlinear Optical Crystal with Strong Second Harmonic Generation Response and Wide Transparency Range, *Angew. Chem. Int. Ed.*, 2021, **133**, 23508-23514.
4. H. Yu, J. Young, H. Wu, W. Zhang, J. M. Rondinelli and P. S. Halasyamani, Electronic, Crystal Chemistry, and Nonlinear Optical Property Relationships in the Dugganite $A_3B_3CD_2O_{14}$ Family, *J. Am. Chem. Soc.*, 2016, **138**, 4984-4989.
5. H. W. Yu, W. G. Zhang, J. Young, J. M. Rondinelli and P. S. Halasyamani, Bidenticity-Enhanced Second Harmonic Generation from Pb Chelation in $Pb_3Mg_3TeP_2O_{14}$, *J. Am. Chem. Soc.*, 2015, **138**, 88-91.
6. S. G. Zhao, Y. Yang, Y. G. Shen, B. Q. Zhao, L. N. Li, C. M. Ji, Z. Y. Wu, D. Q. Yuan, Z. S. Lin, M. C. Hong and J. H. Luo, Cooperation of Three Chromophores Generates the Water-Resistant Nitrate Nonlinear Optical Material $Bi_3TeO_6OH(NO_3)_2$, *Angew. Chem. Int. Ed.*, 2017, **56**, 540-544.
7. Y. G. Chen, N. Yang, X. X. Jiang, Y. Guo and X. M. Zhang, $Pb@Pb_8$ Basket-like-Cluster-Based Lead Tellurate-Nitrate Kleinman-Forbidden Nonlinear-Optical Crystal: $Pb_9Te_2O_{13}(OH)(NO_3)_3$, *Inorg Chem*, 2017, **56**, 7900-7906.